

**UNCLASSIFIED**

---

---

**AD 272 241**

---

*Reproduced  
by the*

**ARMED SERVICES TECHNICAL INFORMATION AGENCY  
ARLINGTON HALL STATION  
ARLINGTON 12, VIRGINIA**



---

---

**UNCLASSIFIED**

NOTICE: When government or other drawings, specifications or other data are used for any purpose other than in connection with a definitely related government procurement operation, the U. S. Government thereby incurs no responsibility, nor any obligation whatsoever; and the fact that the Government may have formulated, furnished, or in any way supplied the said drawings, specifications, or other data is not to be regarded by implication or otherwise as in any manner licensing the holder or any other person or corporation, or conveying any rights or permission to manufacture, use or sell any patented invention that may in any way be related thereto.

# 272 241

ZPh-094  
Physics Section

272241

APR 11 1961

MICROWAVE STUDIES OF FLOW FIELDS  
AROUND HYPERVELOCITY PROJECTILES

M. Schoonover  
B. Siperly  
W. Short

30 June 1961

351760

360

EE

This work was supported by the Army  
Rocket and Guided Missile Agency,  
Contract No. DA-04-495-ORD-3112.

**GD**

GENERAL DYNAMICS | ASTRONAUTICS

ZPh-094  
Physics Section

MICROWAVE STUDIES OF FLOW FIELDS  
AROUND HYPERVELOCITY PROJECTILES

M. Schoonover  
B. Siperly  
W. Short

30 June 1961

This work was supported by the Army  
Rocket and Guided Missile Agency,  
Contract No. DA-04-495-ORD-3112.

**GD**  
GENERAL DYNAMICS | ASTRONAUTICS

CONTENTS

	<u>Page</u>
ABSTRACT . . . . .	iv
I. INTRODUCTION . . . . .	1
II. BALLISTIC RANGE . . . . .	2
III. TEST SECTION . . . . .	4
A. Construction . . . . .	4
B. Microwave Circuitry . . . . .	7
C. Schlieren System . . . . .	11
IV. CALIBRATION . . . . .	12
A. Rod Measurements . . . . .	12
B. Static and Low-Velocity Measurements . . . . .	16
V. HIGH-VELOCITY MEASUREMENTS . . . . .	17
VI. CONCLUSIONS . . . . .	25

## ILLUSTRATIONS

<u>No.</u>	<u>Title</u>	<u>Page</u>
1.	Location of Convair Section in Hyperballistic Range	3
2.	Range Section - System Axes	5
3.	Range Section Looking Toward the Gun	6
4.	Dimensions of Microwave Antenna	9
5.	The 5 Gc System	10
6.	Rod Calibration, Back-Scattered Signal	14
7.	Rod Calibration, Forward-Scattered Signal	15
8.	5 Gc Signals Reflected from Plastic Models at 1 atm Pressure	18
9.	Ratio of Power Reflected to Power Transmitted as a Function of Time Behind the Model, 5 Gc	20
10.	Decay Half-Life of the Trail as a Function of Velocity	21
11.	Ratio of Reflected Power to Transmitted Power as a Function of Body Diameters Behind the Model, 5 Gc	22
12.	Ratio of Transmitted Power with Trail to Transmitted Power without Trail as a Function of Body Diameters Behind the Model, 5 Gc	23
13.	Ultraviolet Radiation from Projectile and Wake (Photomultiplier Uncalibrated)	24

# MICROWAVE STUDIES OF FLOW FIELDS AROUND HYPERVELOCITY PROJECTILES

M. Schoonover  
B. Siperly  
W. Short

## ABSTRACT

↓  
The flow surrounding hypersonic bodies in the atmosphere is studied experimentally and theoretically to explain the observable properties of re-entry nose cones. The experimental studies were performed in a ballistic range using blunt plastic models traveling at velocities up to 26,000 ~~ft/sec~~<sup>f.p.s.</sup>. The bodies and their wakes were observed with microwave equipment at ~~two~~<sup>2</sup> frequencies, a schlieren system and an ~~ultraviolet~~<sup>UV</sup> detector. Approximately 300 microwave measurements of hypersonic projectiles were made. The measurements were reproducible and varied in a consistent manner with respect to velocity and ambient pressure. What appeared to be a transition from laminar to turbulent flow in the wake was detected at 1 mm Hg. Several continuous records of the growth of turbulent wakes at higher pressures were obtained with the schlieren system. The relative ultraviolet emission was measured during the three highest velocity tests.

The theoretical analysis required to compute the number of electrons per unit length of wake was completed, ~~and is being~~ ~~applied to the experimental data~~. It was also shown theoretically that the electron concentration as a function of radial distance in the wake can be computed from microwave reflections at several frequencies. The exact number of frequencies required is not known; however, the calculation will be attempted using the measurements made at four frequencies by Convair and Lincoln Laboratories.

## I. INTRODUCTION

The properties of hypersonic wakes are being investigated by using microwave and schlieren diagnostics. This experimental study was initiated at Convair in 1959 as a basic study of ionization processes in hypersonic flow. The Army Rocket and Guided Missile Agency has supported this work since May 1960 to obtain information concerning observable re-entry phenomena. In this report the construction and operation of the experimental equipment will be described. Samples of the data obtained are presented. The amount of experimental data is too large to include in its entirety; however, it is being reduced, correlated with available theories, and compared with the work of other investigators. The axial distribution of electrons in the wake of a particular type of projectile was derived from the microwave measurements. The rate of growth of turbulent wakes behind variously shaped bodies was determined from the schlieren photographs. The most interesting results are obtained from microwave and schlieren data obtained simultaneously during a single firing. It appears from the phase shift in the microwave returns that the wake, as seen by the microwave signals, expands at the same rate as the turbulent core observed in the schlieren photographs. These results will be presented in later reports.

The experiments were performed in the hyperballistic range at the NASA Ames Research Center. Convair constructed test apparatus which was installed as an integral section of the controlled-atmosphere range. This section contains five antennas for transmitting and receiving 5-Gc and 35-Gc\* signals. In this manner the power propagated through and reflected from projectiles and their ionized wakes can be determined at two frequencies. These frequencies were chosen because measurable transmission through the wake is obtained with the 35-Gc beam at the highest electron concentration expected in the wake, while the 5-Gc beam gives information in regions of low electron concentration. A schlieren system is also contained in the test section.

---

\*Gigacycles -  $10^9$  cycles/sec.

A flash lamp and high-speed framing camera are coupled to the schlieren system to give a record of the density gradients throughout the wake.

## II. BALLISTIC RANGE

The range section used in the experiment is located after the second blast sphere, but before the main range, and is 20 feet from the muzzle of the gun. The location of this section with respect to other range equipment is shown in Figure 1. Baffles in the blast spheres deflect the propellant gas from the gun, so as not to interfere with experiments further downrange.

A variety of light-gas and conventional guns are in use at the Ames Research Center. A shock-heated, light-gas gun was used in the majority of the tests described here. This gun is a 3-stage gun that utilizes a shock wave to compress the gas for propelling the model. At present, the firing rate of the shock-heated gun is about four tests per week. The maximum velocity capability of the gun is approximately 8 km/sec for a 20-mm projectile weighing 5 gm, using hydrogen as the propellant gas.

A modified 20-mm aircraft cannon is available for attaining velocities up to 2.5 km/sec. This gun can be fired at a high rate and is used primarily for calibrating equipment. The projectiles used in both of these guns are 20 mm in diameter and vary from 10 to 25 mm in length. Most models fired have been of three general classes: cone-spherical nose with a cylindrical body, spherical nose with a cylindrical body, and spherical. The flight paths of most projectiles are very close to the axis of the range. The displacement from the axis is usually less than 2 cm. Coordinates of the trajectory are derived from numerous pictures obtained by the shadowgraph stations along the range and the schlieren system in the Convair section. The orientation and condition of the model is also ascertained from the pictures.

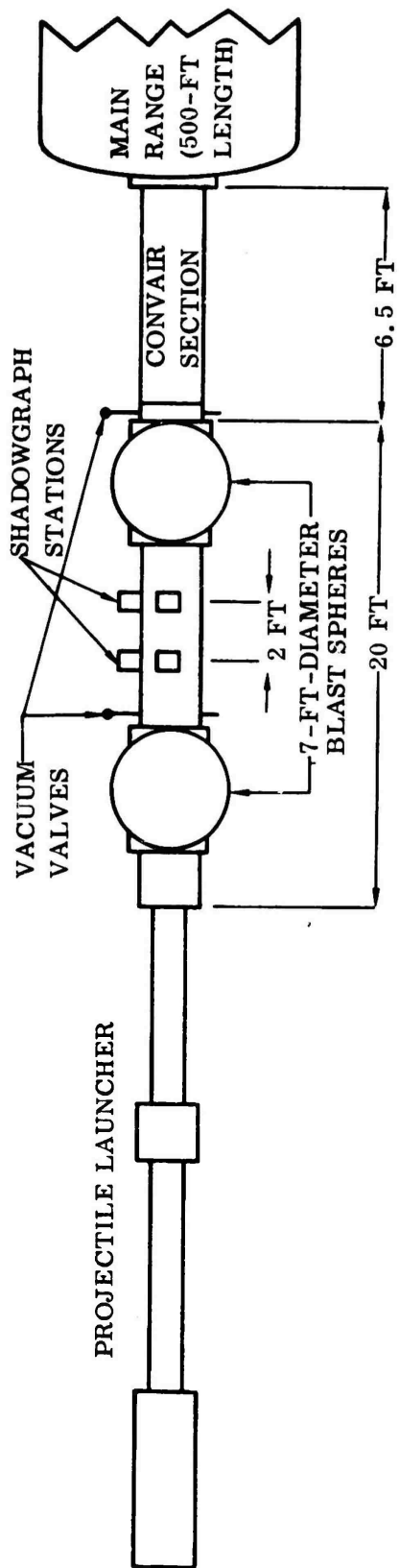


Figure 1. Location of Convair Section in Hyperballistic Range

### III. TEST SECTION

#### A. Construction

The Convair section contains microwave equipment, photo-beam triggering systems, optical monitoring systems, and a schlieren system. A sketch of the section is shown in Figure 2. The section has an overall length of 158 cm and an inner diameter of 48.2 cm. A pressurized slip joint is located at the upstream end to facilitate installation in the range. A sliding valve is located at the upstream flange to isolate the main range from the gun. At present, the vacuum capability of the range is about  $10^{-3}$  atmosphere. All ports are provided with double O-rings. Incorporation of a catcher at the downstream end of the section would enable a much higher vacuum to be achieved than in the range as a whole. Two pairs of diametrically opposed ports contain horns for transverse microwave measurements at 5 and 35 Gc. Both pairs of ports are located with their axes within the field of view of a schlieren system to enable a correlation to be made between microwave data and schlieren photographs of projectiles and wakes. Two additional ports are located upstream of the 5- and 35-Gc ports for Doppler and radar cross-section measurements of a nearly head-on aspect angle. A photomultiplier and filter installed in a 13-cm port near the center of the section are used for measurement of ultraviolet emission. Two pairs of ports are provided for photo-beam trigger units which sense the passage of the projectile by the interruption of a light beam. At present, only one pair is being used while the other pair is used for static microwave measurements of the models. All waveguide entries into the range section are fitted with pressure windows. A flexible waveguide is used near the tunnel section to isolate the microwave components from mechanical shocks induced in the range. The interior of the range section is painted a dull black and lined with a 10-cm-thick microwave absorber to reduce internal reflections. The physical layout of the range section looking toward the gun is shown in Figure 3.

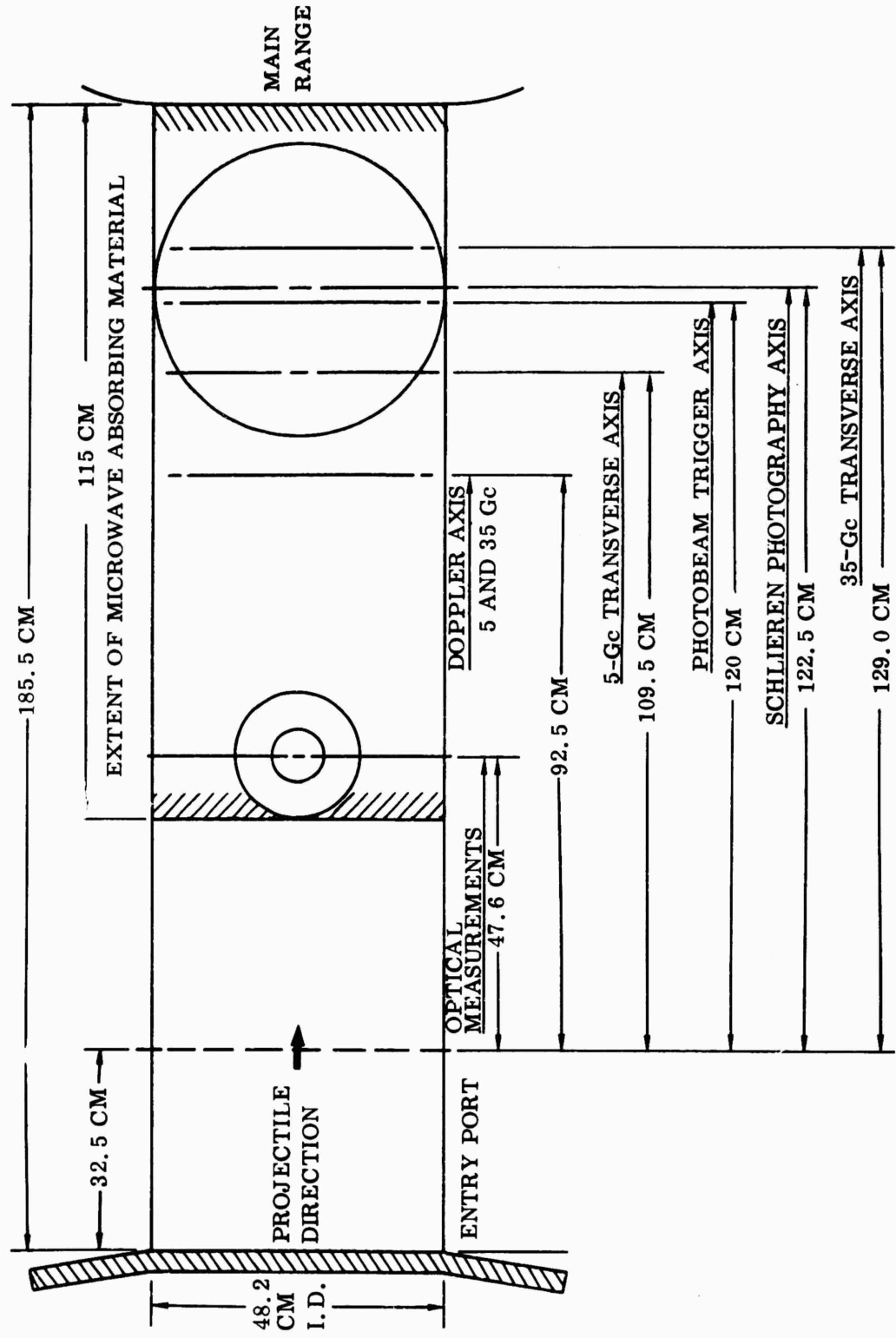


Figure 2. Range Section - System Axes

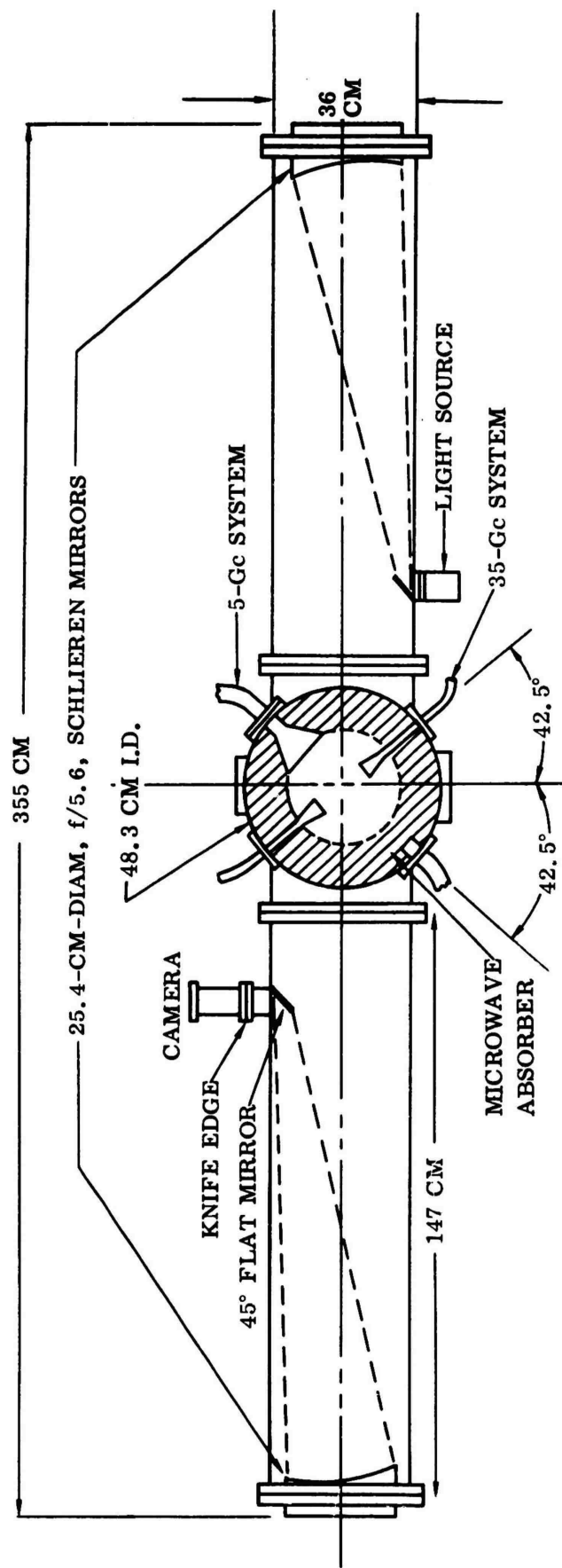


Figure 3. Range Section Looking Toward The Gun

The 5-Gc system uses a wide flare horn as a transmitter with a Teflon lens to correct the phase and produce a plane wave at the trajectory axis. The transmitting horns also receive the reflected or "back-scattered" signals. The receiving or "forward-scatter" aperture is an open-ended waveguide. The transmitting and receiving antennas for the 35-Gc system are identical horns without lenses. In both systems an absorber is placed over the forward-scatter apertures to reduce the reflections caused by scattering from the receiving horn. The dimensions of the antennas are given in Table 1 and Figure 4. The microwave beams are horizontally polarized (the electric vector parallel to the projectile flight path).

#### B. Microwave Circuitry

The two microwave systems are essentially the same. Therefore, the description of the 5-Gc system which follows applies to the 35-Gc system as well. A klystron tuned to the center of the dominant mode serves as a signal generator. A 3-db hybrid junction facilitates division of the power to the transverse and nose-on subsystems. The portion used for transverse measurements is injected into a magic tee, which acts as a duplexer to isolate the receiver branch designated  $P_r$  in Figure 5. Most of the power is passed to the transmitting horn. The energy reflected back into the transmitting horn by the passage of a projectile returns along the same path but is split equally at the magic-tee. One-half the power goes to crystal  $P_r$  and the other half to the hybrid junction. Part of the reflected power is coupled to the transverse Doppler crystal,  $P_d$ , which beats with the transmitted signal to provide phase information. The signal transmitted through the wake is detected by the crystal,  $P_t$ , on the opposite side of the test section. All crystal outputs are presented on oscilloscopes and recorded photographically. The crystal designated  $P_o$  in Figure 5 is a monitor of the power being radiated and provides the reference needed to obtain reflection coefficients.

TABLE 1. Dimensions of Antennas\*

System	C-Band	Ka-Band		
Frequency	5 Gc	35 Gc		
Wavelength	6.0 cm	0.86 cm		
Antenna	Transmitting	Forward-Scatter	Transmitting	Forward-Scatter
Type	Horn with Lens	Waveguide	Horn	Horn
R(cm)	16.5	21.5	7.6	11.4
b(cm)	13.03	2.21	0.95	0.95
c(cm)	15.70	4.75	1.90	1.90
h(cm)	12.2	N/A	8.7	8.7
Antenna Gain, G	36.0		23.6	23.6
Axis to Radiating Point (cm)	19.4		7.6	

\* Figure 4 is a sketch of the antennas, showing the dimensions listed in the above table.

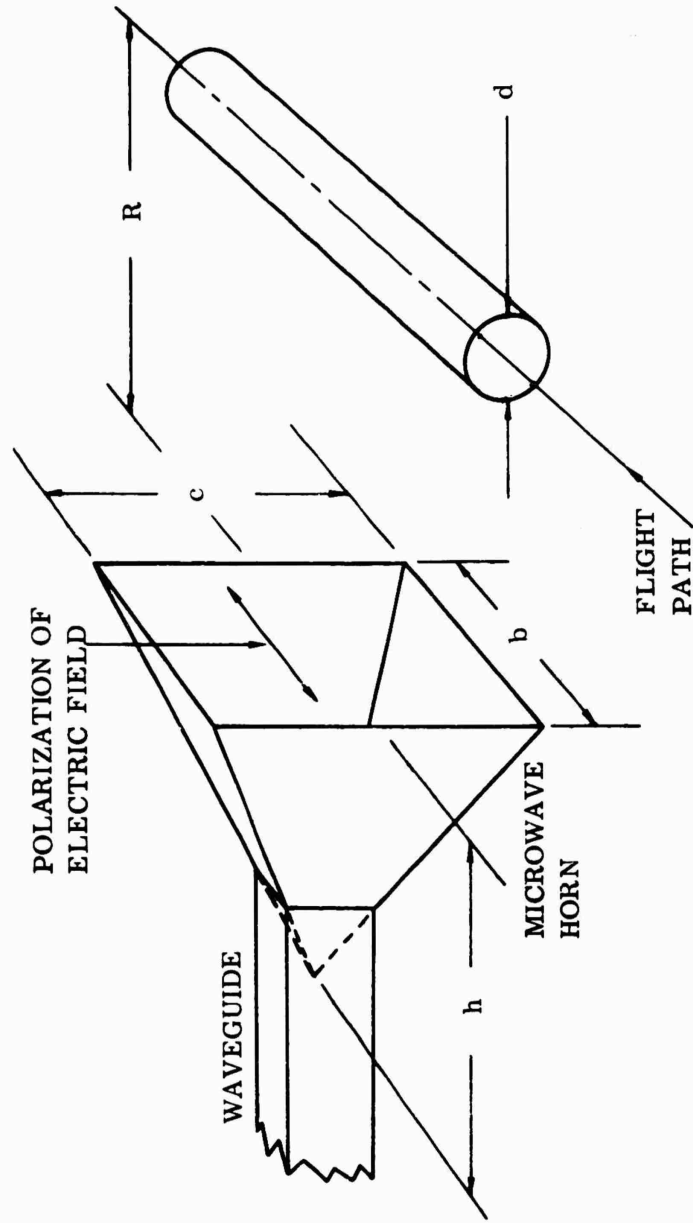


Figure 4. Dimensions of Microwave Antenna

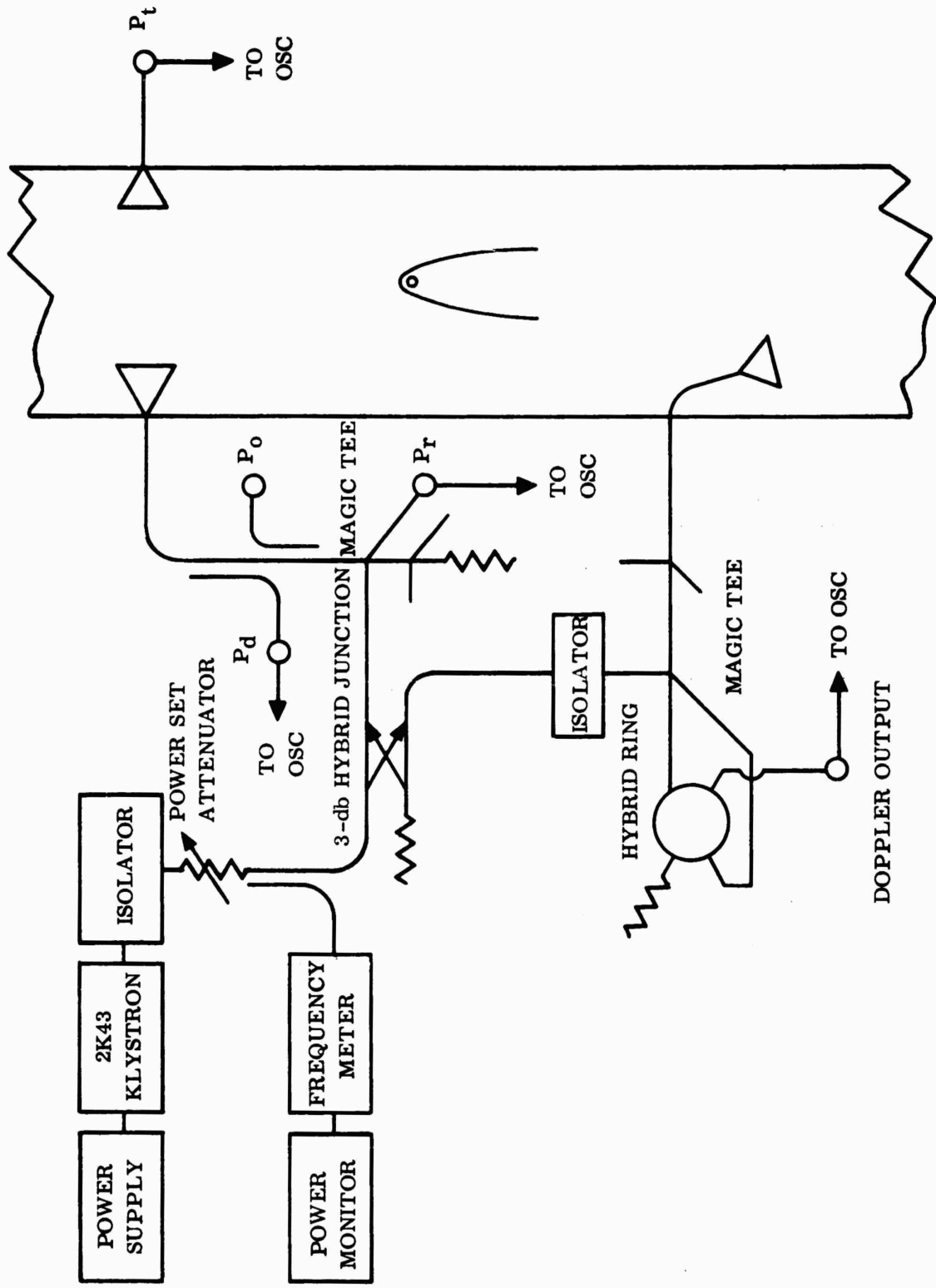


Figure 5. The 5-Gc System

The power taken at the 3-db hybrid junction to power the nose-on measurements is split at a magic-tee as in the transverse system. One-half of the power is radiated toward the model in the range while the other half is applied to a hybrid ring. As in the transverse system, the reflected signal returns through the transmitting waveguide to the tee and is split. One-half the reflected signal is mixed in the hybrid ring with a portion of the transmitted signal. The resulting Doppler signal is detected and recorded.

All oscilloscopes are triggered at the proper time by the photo-beam units and the delay circuits within each scope. Based on the predicted projectile velocity, the time delays and sweep rate are set to record the desired information.

### C. Schlieren System

The schlieren system is a two-element, normal-sensitivity system. The arrangement of the optics is shown in Figure 3. The two 25.4-cm-diam,  $f/5.6$  mirrors are contained in the steel tubes protruding from either side of the range section. The concave mirrors, the small deflecting mirrors, and the knife edge can be adjusted while the range is evacuated. To obtain high sensitivity with this system, fine adjustments must be made after the range is evacuated because slight distortions occur during evacuation.

The sensitivity of the system was checked by diffracting part of the light in the field of view through a very small but known angle by means of two prism devices inserted at the test plane. By rotating one prism, angular deviations of light between 0 and 10 sec of arc normal to the knife edges were produced. When the system is properly adjusted, light-ray deviations of one-tenth sec of arc are observable. Deviations of 5 sec completely darken the field.

In the range, spark-schlieren photographs can be obtained at a pre-selected time with respect to the model passage by using a photobeam and delay circuit located 2.5 cm upstream from the schlieren axis. This method of operation produces a very clear picture of the projectile or

a section of the wake on Polaroid film or 4- by 5-in. negatives.

A second method of operation which employs a framing camera provides more complete information concerning the wake at the expense of clearness and resolution. A Beckman-Whitley framing camera was used to obtain continuous records of the wake. At the highest framing rate, 26,000 frames per sec, overlapping 10-in. fields of view were obtained of projectiles traveling 5.5 km/sec. The exposure time of the Beckman-Whitley camera is adjustable to 1, 2, or 5  $\mu$ sec per frame.

Firings at several pressures between 1 atm and 1 mm Hg have been observed. Very clear pictures of the bow shock, secondary shock, and the turbulent wake can be obtained at 1 atm and at all velocities up to 6 km/sec. Some density gradients in the inviscid wake outside the turbulent core can be observed. At 20 mm Hg and projectile velocities of 6 km/sec, the turbulent wake is still visible; however, the outline of the core is diffuse.

At 1 mm Hg the shock waves are still visible in the spark-schlieren photographs; however, the turbulent wake is not discernible.

#### IV. CALIBRATION

##### A. Rod Measurements

Numerous tests and theoretical studies have been conducted in order to understand the microwave fields in the Convair Range section. These tests explore the field amplitude and phase in detail to better interpret experimental results obtained during high-velocity firings. Effects such as amplitude variations within the propagated beam, cavity excitation, curvature of the wave front, and internal reflections from walls and equipment mounted in the range could seriously affect the observations. The resonant frequencies of the cylindrical test section were computed.<sup>1</sup> It

---

1. G. Plato, "Calculation of the Resonance Frequencies of a Cylindrical shell," Convair, San Diego, Calif., Ph-121-M, May 1961.

was concluded that resonant frequencies near the transmitted frequency could exist; therefore, heavy absorbing material is desired in the range. Conducting rods were inserted at the axis of the range, and the microwave returns from these rods were recorded. The returns from infinitely long, cylindrical conductors can be predicted theoretically. Therefore, before attempting the more complicated analysis of ionized wakes, the theoretical and experimental techniques were tested using rods.

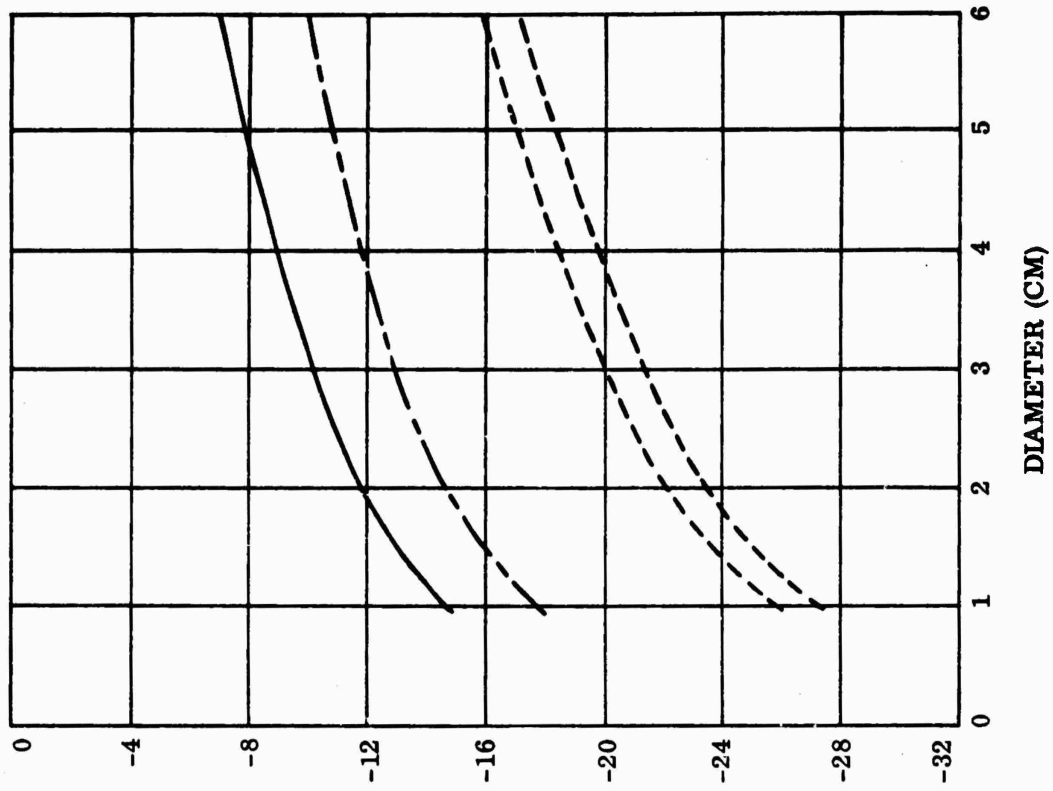
Figures 6 and 7 present the forward-scattered and the back-scattered signals obtained from metal rods at 5 and 35 Gc. The signals are plotted in terms of the power ratios  $P_r/P_o$  and  $P_t/P_1$  in decibels, where:  $P_o$  is the power emitted by the transmitting antenna;  $P_r$  is the power reflected into the transmitting antenna;  $P_1$  is the power received by the forward-scattered antenna without a rod in place; and  $P_t$  is the power received by the forward-scattered antenna with the rod in place. The broken lines in the figures indicate the scatter of the experimental data. Theoretical curves for the back-scattered data assuming both a plane- and spherical-transmitted wave are included. The theoretical calculation of reflected power ratios is based on geometric optics which predicts

$$\frac{P_r}{P_o} = \frac{d}{4R}$$

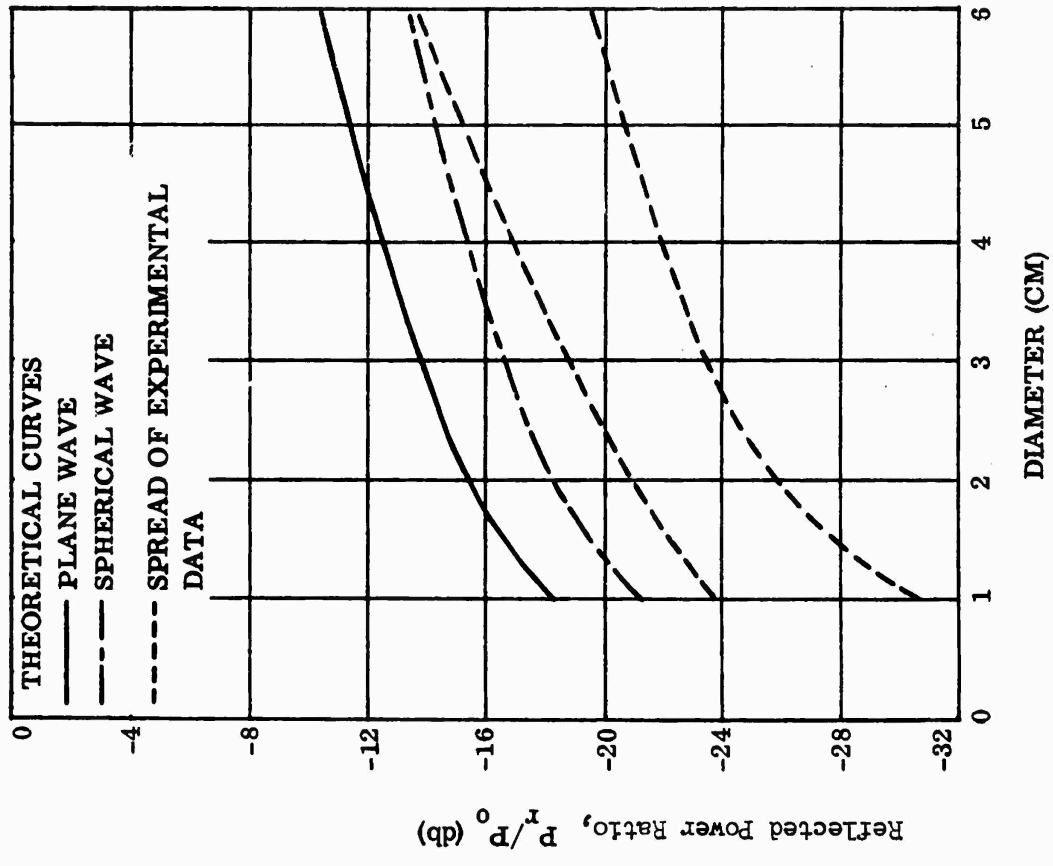
for a plane wave and

$$\frac{P_r}{P_o} = \frac{d}{8R}$$

for a spherical wave. The applicability of geometric optics for predicting reflected signals when the rod size is comparable to the wavelength of the radiation is doubtful. This technique cannot be used for the forward-scattered signal because the antenna is in the shadow. A theory appropriate for the geometry used is being investigated for future use.



a. 5-Gc Signal



b. 35-Gc Signal

Figure 6. Rod Calibration, Back-Scattered Signals

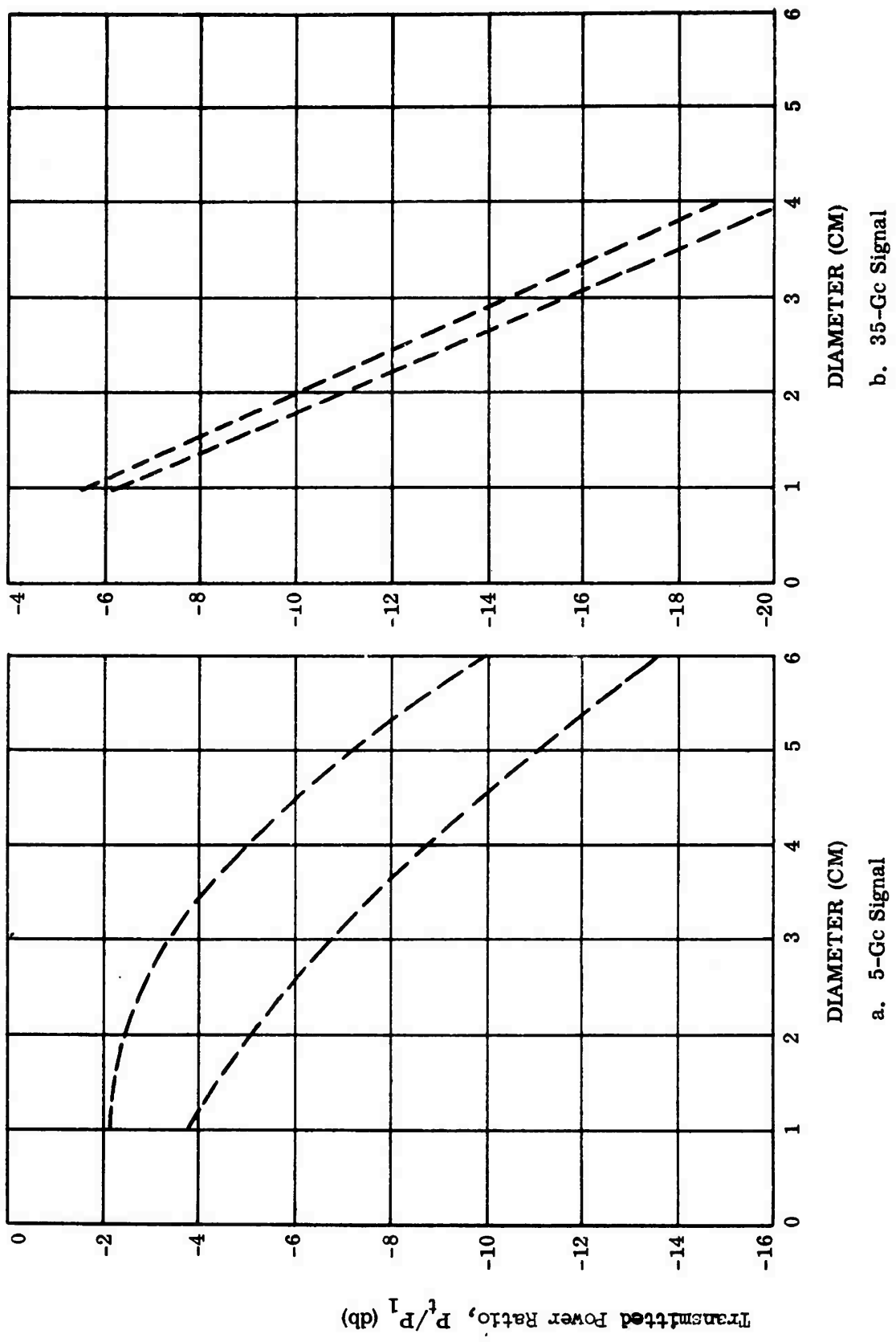


Figure 7. Root Calibration, Forward-Scattered Signals

As shown by the dashed curves in Figures 6 and 7, there is considerable scatter in the experimental data. Several reasons for this variation can be given. First, the rods are held at the trajectory axis by a dielectric cone at each end of the rod. A variation in the amount of pressure holding the cones against the ends of the cylinder causes a change in the signals. This may be due to standing waves produced on the rod because the electric vector of the radiation is oriented parallel to the axis of the rod. Changing the pressure against the ends results in a variable-capacity termination and variation in the standing waves. A test to simulate more adequately an infinitely long, conducting cylinder is necessary. This could be done by suspending a rod having properly tapered end sections at the axis of the range. The smaller rods are well within the Rayleigh region of scattering; therefore, a slight variation in the placement of the rod results in a large variation in scattered signal. Returns from a given rod may vary by a factor of 10 from test to test when the rods are not positioned carefully. However, variations were reduced to a factor of about 3 by careful positioning of the rods.

#### B. Static and Low-Velocity Measurements

Experiments were performed with aluminum spheres, nylon spheres, and the polyethylene models used in the high-velocity shots to determine the beam widths, the return from models without an ion sheath, and the effective radiating point of the transmitting antennas. To obtain static returns the models were mounted on a string by means of holes drilled along their axes of symmetry. The string was stretched along the flight path in the test section and the models were pulled past the microwave horns. The "static" measurements were actually made at velocities near 10 cm/sec. Low-velocity data refers to that derived from models fired at 1.5 to 2.3 km/sec from the powder gas gun. At 1.5 km/sec the forward-scattered signals are identical to those obtained by the "pull-through" method, whereas the reflected signals differed slightly. The models launched from the gun gave smoother signals than those pulled through

because the fired models did not oscillate off-axis while passing through the test section. Figure 8 shows the 5-Gc signals reflected from models propelled by both techniques. The range pressure was atmospheric and the models were polyethylene cylinders, 2 cm in diam by 1 cm long with a 1.5-cm-radius forward face. The static measurement (12.6 cm/sec) indicates the beam width is approximately 20 cm at the axis. Based on other measurements, the beam widths of the 5- and 35-Gc transmitting horns were found to be 31 and 16 deg, respectively, at the 3-db point. The increase in cross section of the model caused by ionization of air at velocities above 1.5 km/sec, as well as the beginning of an ionized trail, can be observed in Figure 8. Initially, all low-velocity measurements were made in air at one atmosphere pressure. Recent tests have been conducted at reduced pressures, in order to learn whether the trail returns were caused by propellant gases following the model, ablation products caused by heating of the model in the gun, or an ionized wake. Firings have been made down to a pressure of 66 mm Hg with sabotaged models to prevent heating in the barrel. The evidence indicates that it is an ionized wake created at low velocities which is being detected by the microwave systems.

#### V. HIGH-VELOCITY MEASUREMENTS

The Ames Range has recently attained projectile velocities up to 8 km/sec in air at 1 mm Hg pressure. The reflected power ratios obtained during the high-velocity firings are plotted in Figure 9 as a function of time after the model passes the antenna axis. The models were the same polyethylene models used during the low-velocity calibrations discussed in the preceding section. The decay of the reflected signals is approximately linear (Figure 9) during the first 100  $\mu$ sec. The ordinate is measured in decibels, which is a logarithmic scale. Hence, the characteristic decay time selected to describe each curve is the half-life, which is the time for the power ratio to decrease by one-half. The initial half-life for each test is plotted in Figure 10.

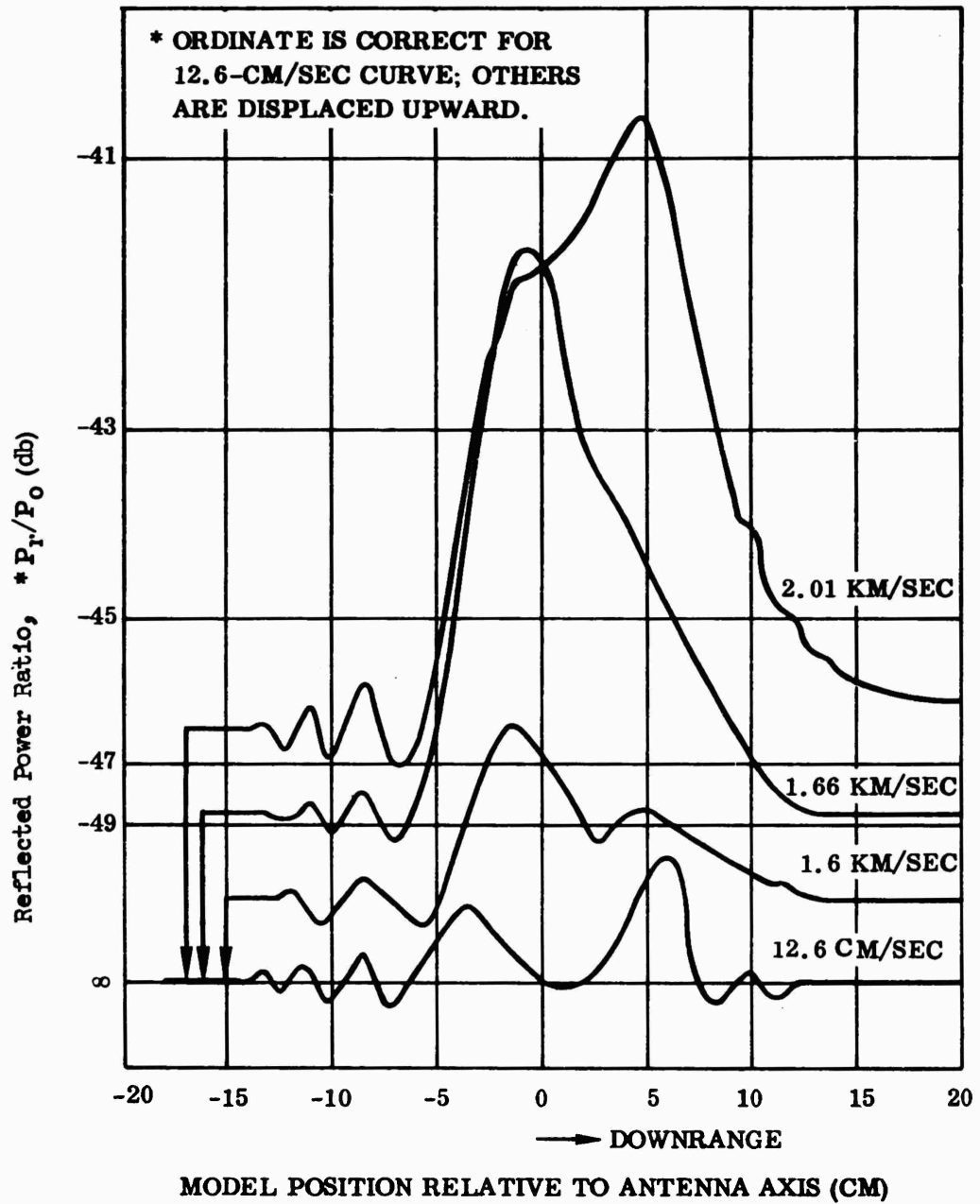


Figure 8. 5-Gc Signals Reflected from Plastic Models at 1 Atm Pressure

The results of the data obtained indicate an abrupt change in the half-life at approximately 5.67 km/sec. This may be the transition from laminar to turbulent flow which is known to occur at these pressures. About 400  $\mu$ sec after the projectile passes the antenna, some curves in Figure 9 begin to increase. Schlieren photos taken with the Beckman-Whitley Dynafax camera show the cause of this increase. One foot downstream from the C-band horn, the model enters the main range through a 6-in.-diam hole in the end plate. The schlieren photos show that the bow shock wave is reflected from this end plate. This causes a temporary increase of electron density in the microwave beam. (The plate has subsequently been covered with an absorbing material to reduce the strength of the reflected shock.)

The data gained during three high-velocity shots will be discussed in detail. These shots are designated by the numbers 145, 146, and 147, and have velocities of 6.61, 7.81 and 7.60 km/sec, respectively. The microwave and optical characteristics of these shots are presented in Figures 11, 12, and 13. It may appear from the maximum in the curves that the model crossed the antenna axis as much as 15 diameters later than indicated by the ordinate. The greatest reflection occurs near the model because the flow is highly ionized in this region. However, the received signal is an integrated effect and is related to the total number of electrons in the antenna field; therefore, the maximum return probably occurs as the projectile is just leaving the field. The C-band beam is about 20 cm wide at the range axis, and at a velocity of 7.6 km/sec, the projectile requires 27  $\mu$ sec to pass through it. Therefore, the maximum return would occur 5 diameters behind the model. This is in fair agreement with the curves in Figure 11. It is believed that the beginning of the smooth exponential decay occurs when the ionized wake spans the distance across the beam. Figure 6a shows that the initial reflection from the wake (-17 db) corresponds to the reflection obtained from a metal rod of about 6-cm diam.

The receiving antenna is an open-ended waveguide and, thus, does not

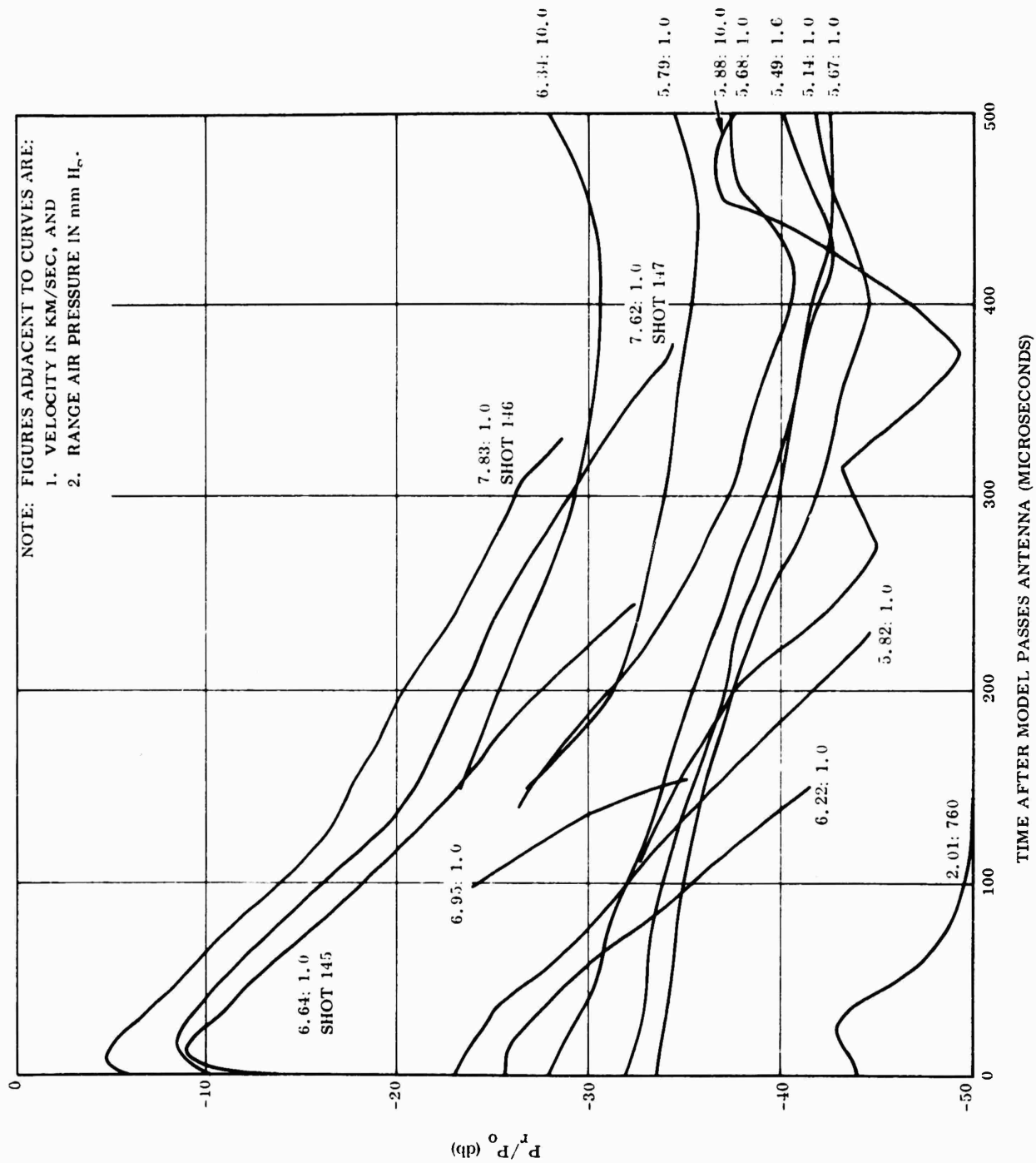


Figure 9. Ratio of Power Reflected to Power Transmitted as a Function of Time Behind the Model, 5 Gc

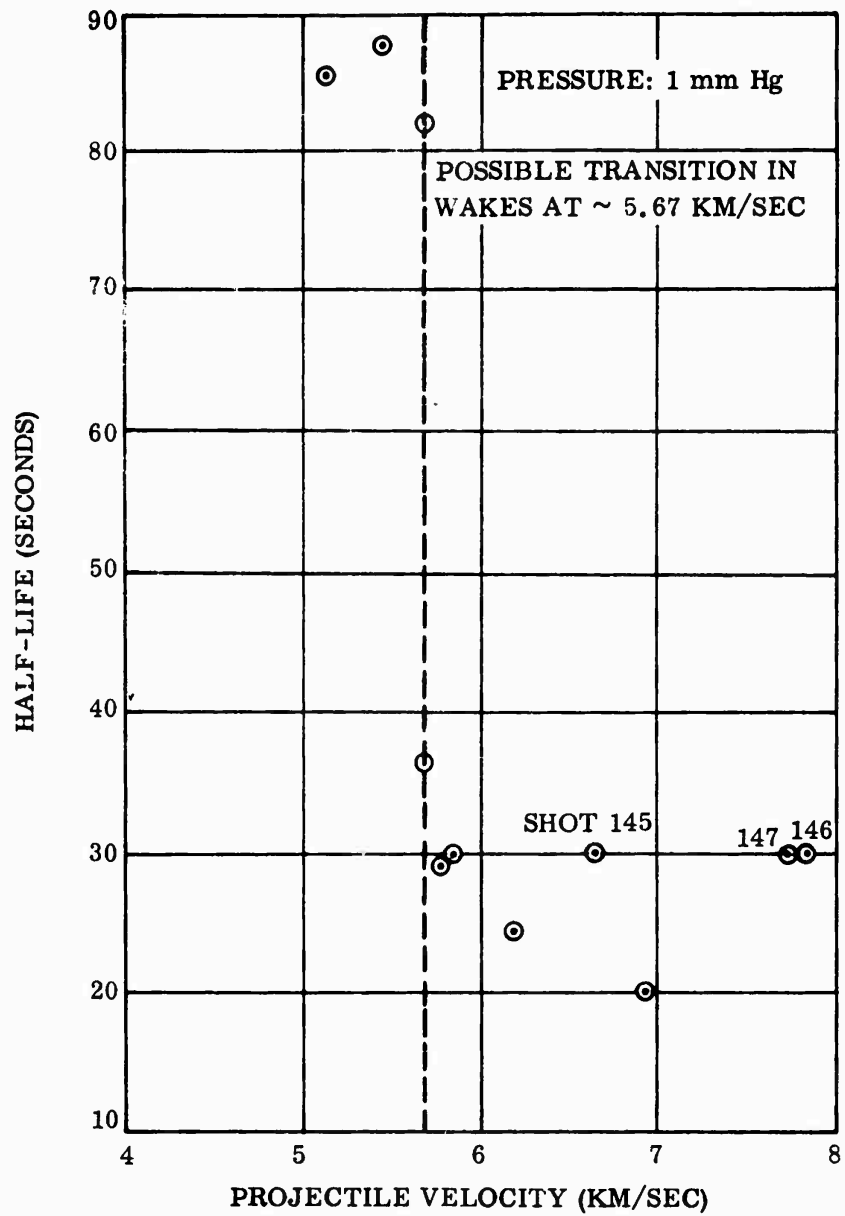


Figure 10. Decay Half-life of the Trail as a Function of Velocity

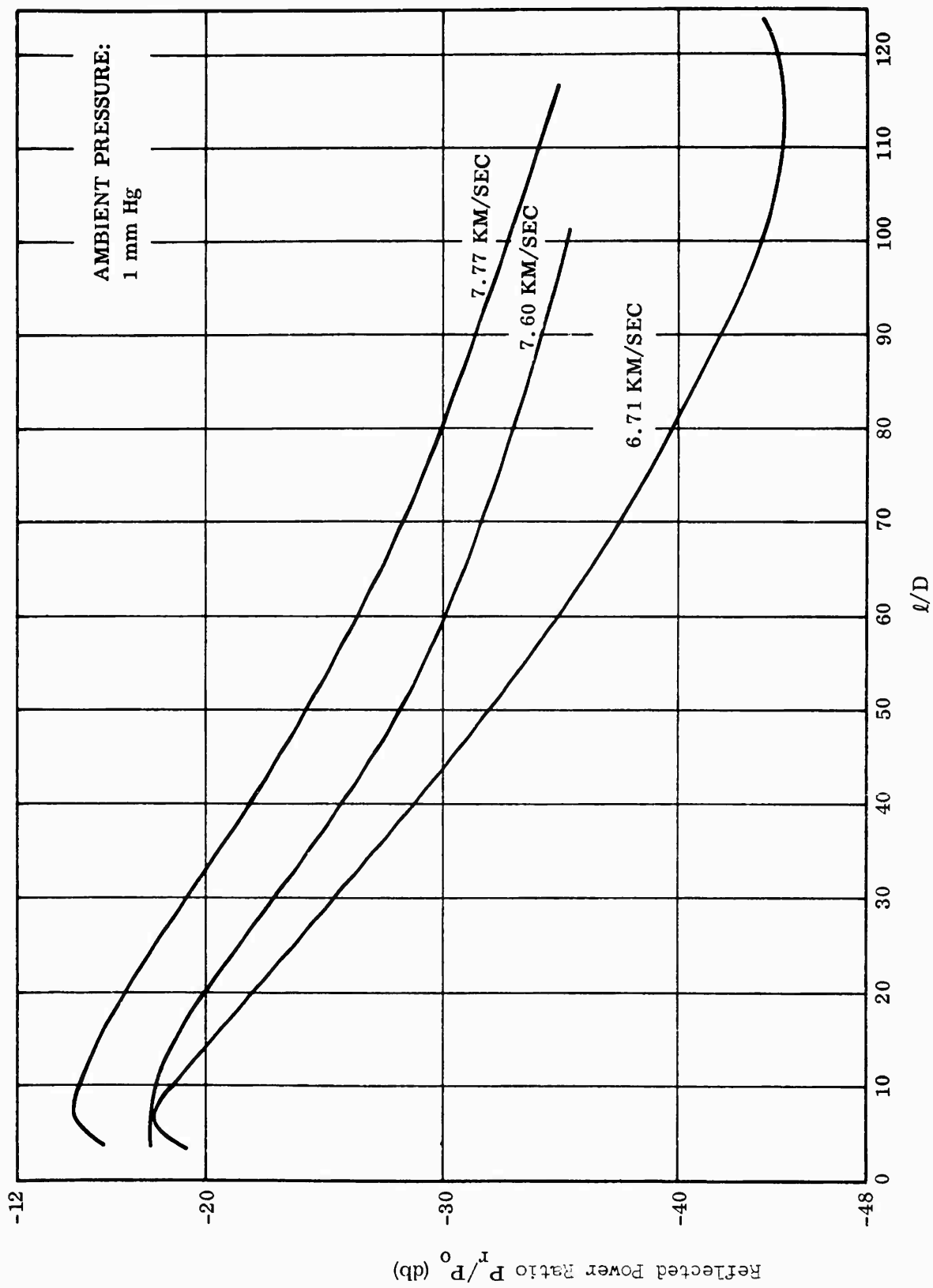


Figure 11. Ratio of Reflected Power to Transmitted Power as a Function of Body Diameters Behind the Model, 5 Gc,  $D = 2$  cm

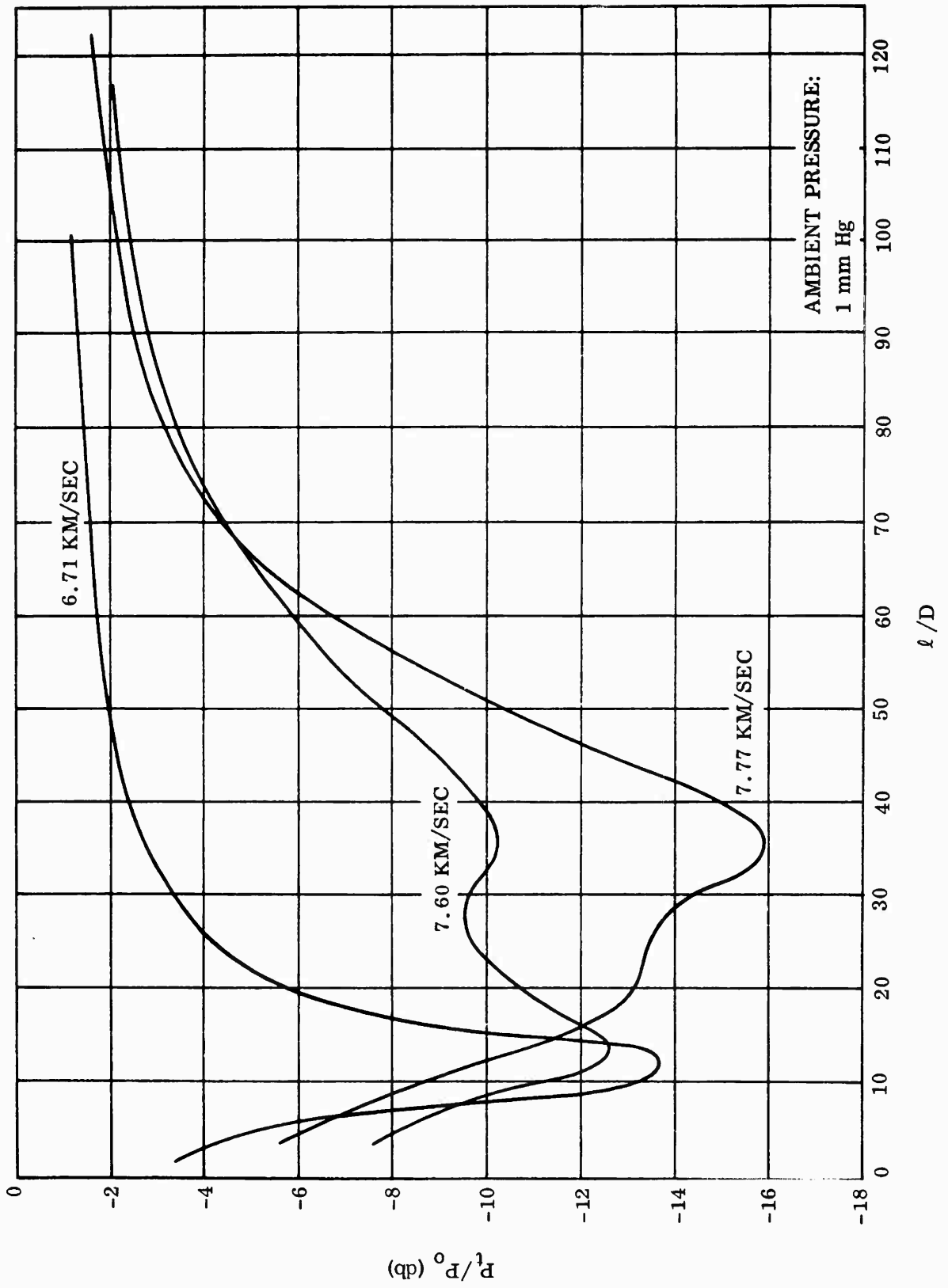


Figure 12. Ratio of Transmitted Power With Trail to Transmitted Power Without Trail as a Function of Body Diameters Behind the Model, 5 Gc,  $D = 2$  cm

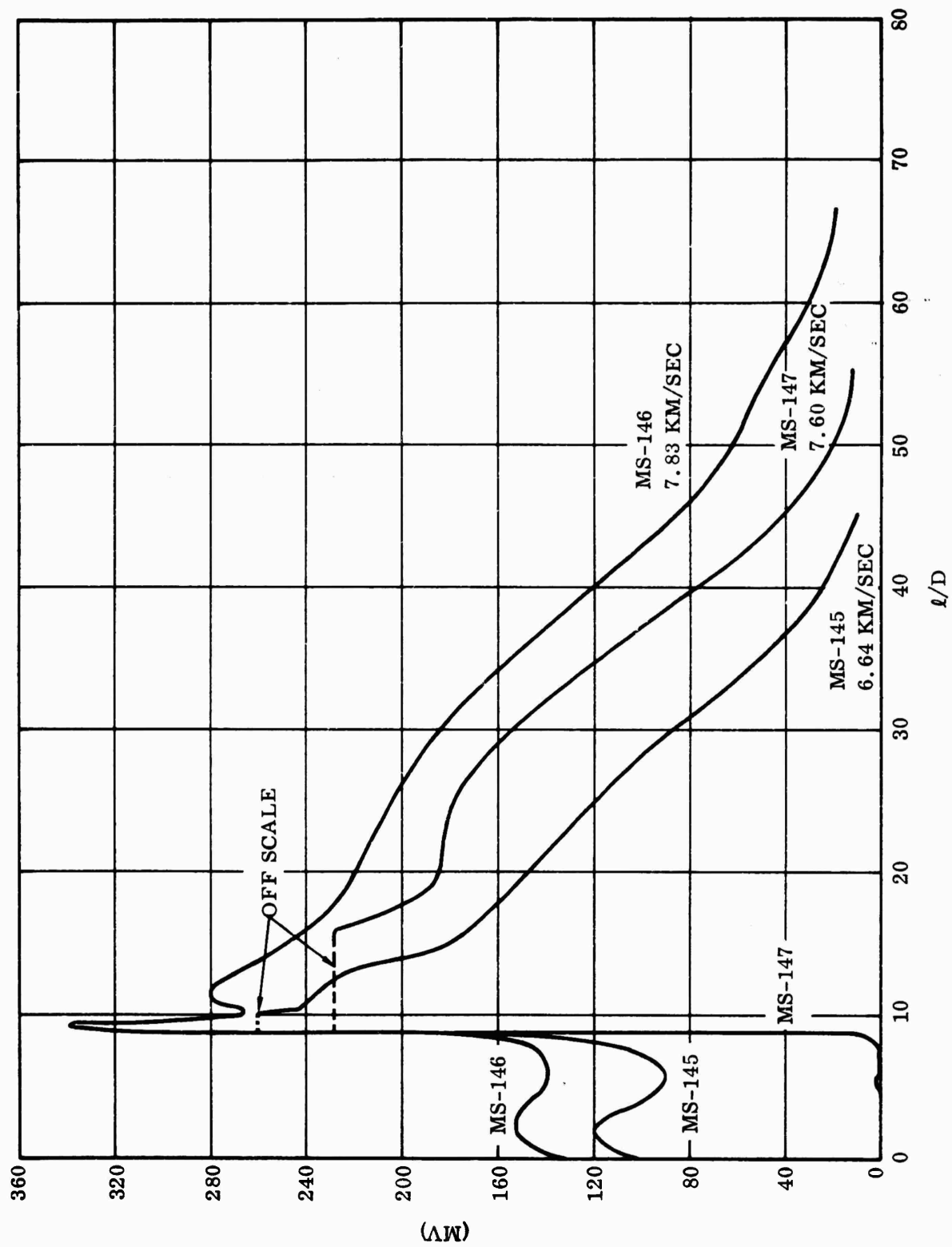


Figure 13. Ultraviolet Radiation from Projectile and Wake (Photomultiplier Uncalibrated),  $D = 2$  cm

have the directional properties of the transmitter. Also, it is situated farther back from the range axis. The effective beam width for the 5-Gc forward receiver is wider than that for the back-scatter antenna. The minimum signal (i.e., greatest attenuation) is attained about the time the projectile leaves the beam. Figure 6b shows that this attenuation (-13 db) is also produced by a metal rod approximately 6 cm in diameter.

It is interesting that the initial magnitudes of both forward- and back-scattered signals are equivalent to that caused by a metal rod approximately 6 cm in diam. On the other hand, farther back in the wake the back-scattered signals decrease smoothly, while the variation of the forward-scattered signals depends strongly on velocity. An explanation for the behavior of these signals is that a region about 6 cm in diam containing electrons in density greater than  $3 \times 10^{11} \text{ cm}^{-3}$  is established about 10 cm behind the projectile. A concentration of  $3 \times 10^{11}$  electrons/ $\text{cm}^3$  is the critical density or the concentration at which 5-Gc radiation is completely reflected. Initially, this region is sharply bounded and reflects 5-Gc radiation much the same as a metal rod, but it rapidly diffuses, forming an absorbing region which strongly reduces the reflected signal. The forward-scattered signal, however, may depend on whether the critical concentration contour increases or decreases in radius.

The ultraviolet radiation emitted as the projectile passed the port 76.4 cm uprange of the schlieren system was measured by a Du Mont 2088 photomultiplier. The filter transmitted between 3300 and 4000 A. The relative intensities for three shots are given in Figure 13. The system was not calibrated to give absolute intensities.

## VI. CONCLUSIONS

It is believed that the laminar-to-turbulent transition in the wake of blunt cylinders used in this investigation occurs at 5.607 km/sec in air at 1 mm Hg pressure. This conclusion is based on the microwave re-

turns from three firings and cannot be considered conclusive. Hildalgo et al.<sup>2</sup> have obtained similar data in a ballistic range using photomultipliers and a drum camera. Their conclusion was that transition occurs behind spheres at 4.6 km/sec in air at 2 cm Hg, and that the transition is insensitive to velocity. The data presented in Figure 10 shows the transition to be sensitive to velocity. The transition point cannot be scaled simply on the basis of a free-stream Reynolds number. However, because the conditions in Hildalgo's experiment and the present experiment differ only slightly, a free-stream Reynolds number correlation will be attempted. Assuming the viscosities are equal and the density is proportional to pressure, the products of body radius, velocity, and free-stream pressure should be identical in the two experiments. The product of these three parameters obtained by Hildalgo is three times that obtained here. This is good agreement in view of the difference in body geometry.

The use of microwave radiation is a very sensitive means of detecting the shape of projectiles and the presence of ionized regions in the flow around projectiles. For example, the lower curve in Figure 8 shows the fore and aft ends of the projectile are not symmetrical. At velocities above 1.5 km/sec ionization can be detected, and the microwave return or cross section increases very rapidly at higher velocities. It is not known whether the large increase in cross section occurring at velocities of 1.6 km/sec is due to an ionization phenomenon associated with this velocity or if the signal merely reaches a detectable level at this velocity. The signal strengths are more than 50 db below the transmitted signal. This means the model reflects  $10^{-5}$

- 
2. H. Hildalgo, R. L. Taylor, and J. C. Keck, "Transition from Laminar to Turbulent Flow in Viscous Wake of Blunt Bodies Flying at Hypersonic Mach Numbers," AVCO R. M. 218, May 1961.

of the transmitted power.

The simple relations developed from geometric optics are unsuitable for analyzing the calibration data obtained by means of the metal rod, or for reducing the wake data. The inadequacies of geometric optics for conducting cylinders result from the microwave energy having wavelengths comparable to the diameter of the rods and wakes observed. A more refined theoretical analysis of the reflection and transmission properties of metal rods is being prepared. The applicability of any theory can be conveniently assessed by comparison with the calibration data.

Barthel has estimated electron concentrations in wakes in several flow regimes<sup>3</sup> and has investigated methods for computing electron density.<sup>4</sup> The reflection or transmission of microwaves by known plasmas can be determined with a high degree of certainty, although the computation for unusual electron distribution may be time-consuming. The inverse problem of computing the electron distribution, knowing the microwave properties, is conceptually more difficult. In the case of dilute plasmas, however, the total number of electrons in the wake can be obtained from an individual electron-scattering theory. The highly ionized or dense plasmas which are encountered in hypersonic wakes present the most difficult analytical problem. A dense plasma is the situation in which the electrons closest to the transmitter highly attenuate the beam or reflect it completely. Barthel<sup>4</sup> has developed a theoretical technique for handling some dense plasmas. The theory involves an integration of properties observed over a wide range of frequencies. The number of frequencies required is not known, but it undoubtedly depends on the accuracy of the data. Lincoln Laboratories and Convair have obtained simultaneous microwave data at four frequencies. These data will be compared to check their consistency, and an attempt will be made to establish the distribution of electrons in wakes.

---

3. J. Barthel, "A Note on Some Investigations of Re-entry Wakes," Convair, San Diego, Calif., Ph-119-M.

4. J. Barthel, "The Microwave Diagnosis of a Column of Ionized Gas," Convair, San Diego, Calif., ZPh-096, May 1961.